*Proc. Natl. Acad. Sci. USA*
Vol. 87, pp. 4675–4679, June 1990
Neurobiology

# The noncompetitive blocker [$^3$H]chlorpromazine labels three amino acids of the acetylcholine receptor $\gamma$ subunit: Implications for the $\alpha$-helical organization of regions MII and for the structure of the ion channel

(channel blockers/ligand-gated ion channels/allosteric proteins)

FRÉDÉRIC REVAH*, JEAN-LUC GALZI*, JÉRÔME GIRAUDAT*, PIERRE-YVES HAUMONT†, FLORENCE LEDERER†, AND JEAN-PIERRE CHANGEUX*

*Neurobiologie Moléculaire, Unité de Recherche Associée au Centre National de la Recherche Scientifique 1284, Institut Pasteur, 25 rue du Dr Roux, 75724 Paris Cédex 15, France; and †Unité 25 de l'Institut National de la Santé et de la Recherche Médicale, Laboratoire Associé au Centre National de la Recherche Scientifique 122, Hôpital Necker, 75730 Paris Cédex 15, France

*Contributed by Jean-Pierre Changeux, March 5, 1990*

ABSTRACT **Labeling studies of *Torpedo marmorata* nicotinic acetylcholine receptor with the noncompetitive channel blocker [$^3$H]chlorpromazine have led to the initial identification of amino acids plausibly participating to the walls of the ion channel on the $\alpha$, $\beta$, and $\delta$ subunits. We report here results obtained with the $\gamma$ subunit, which bring additional information on the structure of the channel. After photolabeling of the membrane-bound receptor under equilibrium conditions in the presence of agonist and with or without phencyclidine (a specific ligand for the high-affinity site for noncompetitive blockers), the purified labeled $\gamma$ subunit was digested with trypsin, and the resulting fragments were fractionated by HPLC. Sequence analysis of peptide mixtures containing various amounts of highly hydrophobic fragments showed that three amino acids are labeled by [$^3$H]chlorpromazine in a phencyclidine-sensitive manner: Thr-253, Ser-257, and Leu-260. These residues all belong to the hydrophobic and putative transmembrane region MII of the $\gamma$ subunit. Their distribution along the sequence is consistent with an $\alpha$-helical organization of this segment. The [$^3$H]chlorpromazine-labeled amino acids are conserved at homologous positions in the known sequences of other ligand-gated ion channels and may, thus, play a critical role in ion-transport mechanisms.**

Reconstitution of the ionic-permeability response to acetylcholine from the purified nicotinic acetylcholine receptor protein (AcChoR) (1) or from its subunits mRNAs (2) showed that this membrane-bound allosteric protein contains the ion channel, the acetylcholine-binding sites, as well as all the structural elements required for their interaction (for review, see refs. 1 and 3). The identification of the ion channel carried by this $\alpha_2\beta\gamma\delta$ pentamer has benefited from labeling studies with a distinct category of pharmacological agents, the noncompetitive blockers (NCBs), which inhibit the ionic response to acetylcholine without significantly binding to the agonist sites. Equilibrium binding experiments on AcChoR-rich membranes from Torpedo marmorata electric organ revealed that these NCBs interact with a high-affinity site, present at a single copy per $\alpha_2\beta\gamma\delta$ oligomer and which selectively binds the hallucinogen phencyclidine (PCP) (ref. 4 and the references therein). When bound to this site, the NCB [$^3$H]chlorpromazine ([$^3$H]CPZ) photolabels all *T. marmorata* AcChoR subunits (4, 5), suggesting that this unique high-affinity site is located along the axis of pseudosymmetry of the receptor molecule (4). Rapid-mixing photolabeling experiments (6) further showed that when the channel is opened by agonists, [$^3$H]CPZ labels its site according to a simple bimolecular mechanism almost diffusion-limited, supporting the notion initially proposed from electrophysiological data (for review, see refs. 7 and 8) that this site lies within the ion channel (see also ref. 9).

To elucidate the structure of the AcChoR ion channel, we have undertaken the identification of the amino acids labeled by [$^3$H]CPZ under equilibrium in a PCP-sensitive manner. We have previously reported the identification of serines-262 of the $\delta$ chain (Ser-$\delta$262), -254 of the $\beta$ chain (Ser-$\beta$254), -248 of the $\alpha$ chain (Ser-$\alpha$248), and leucine -257 of the $\beta$ chain (Leu-$\beta$257) (10–12), which all belong to the second hydrophobic segment of each subunit, MII. Studies using another photolabile NCB, [$^3$H]triphenylmethylphosphonium, have suggested that this compound labels the same serine residues as [$^3$H]CPZ on the $\alpha$, $\beta$, and $\delta$ subunits (13, 14). Finally, site-directed mutagenesis (15–17, 32) has brought complementary information and additional evidence in favor of the notion that segment MII and neighboring amino acids contribute to the regulation of ion transport through the channel.

In the present paper, we demonstrate that on the $\gamma$ subunit of *T. marmorata* AcChoR, three residues belonging to the MII segment are labeled by [$^3$H]CPZ in a PCP-sensitive manner under equilibrium conditions. The implications of these results in terms of a plausible structural model of the AcChoR ion channel are discussed.

## MATERIALS AND METHODS

Live *T. marmorata* were obtained from the Station de Biologie Marine (Arcachon, France). [$^3$H]CPZ was purchased from NEN (20–25 Ci/mmol; 1 Ci = 37 GBq); unlabeled CPZ, carbamoylcholine, and vinylpyridine were from Sigma; L-1-tosylamido-2-phenylethylchloromethyl ketone (TPCK)-trypsin was from Merck, cyanogen bromide was from Kodak. PCP was a gift from A. Jaganathen (Université Louis Pasteur, Strasbourg, France).

Purification and covalent labeling of the AcChoR by [$^3$H]CPZ were performed as described (10). [$^3$H]CPZ was isotopically diluted to 2–3 Ci/mmol for preparation 1 and to 12–14 Ci/mmol for preparation 2. The purified $\gamma$ subunit (10) was carboxymethylated (10) or pyridylethylated (18) and finally precipitated twice with acetone after desalting.

Information concerning tryptic cleavage, peptide fractionation, and sequencing are given in figure legends.

The publication costs of this article were defrayed in part by page charge payment. This article must therefore be hereby marked "*advertisement*" in accordance with 18 U.S.C. §1734 solely to indicate this fact.

Abbreviations: AcChoR, nicotinic acetylcholine receptor; NCB, noncompetitive blocker; CPZ, chlorpromazine; PCP, phencyclidine; PTH, phenylthiohydantoin.

## RESULTS

**Labeling of the γ Subunit by [$^3$H]CPZ.** Large batches of alkali-treated AcChoR-rich membrane fragments (≈200 nmol of α-toxin binding sites) were photolabeled by [$^3$H]CPZ in the presence of 1 mM carbamoylcholine under equilibrium conditions. All AcChoR subunits were labeled, and a 200 μM concentration of PCP reduced the radioactivity incorporation in all subunits (60–65% for the γ subunit). The subunits derived from labeled membranes were purified by preparative SDS/PAGE without detectable loss of covalently bound [$^3$H]CPZ. Analysis of the radioactivity in the purified material showed that ≈2% of the γ subunits were labeled by [$^3$H]CPZ in a PCP-sensitive manner.

**Analysis of the Carboxymethylated γ Subunit Tryptic Fragments.** The purified carboxymethylated γ subunit from preparation 1 (specific radioactivity, 87,000 dpm/nmol of γ subunit vs. 30,100 dpm/nmol for the PCP-protected batch) was cleaved with trypsin, and the digest was fractionated by reversed-phase HPLC (Fig. 1). Approximately 20% of the injected radioactive material eluted with the unbound species. The radioactivity in the corresponding fractions of the PCP-protected sample did not decrease; these fractions were not further analyzed.

Sixty-five percent of the injected radioactivity was recovered associated with a broad $A_{230}$ peak, eluting between 38% and 77% solvent B (see Fig. 1 legend). This material was subdivided into two pools, I and II, corresponding to peptides eluting respectively between 38–48% and 48–78% solvent B. The radioactivity of pool I was reduced by 35% in the PCP-protected batch, whereas it was reduced by 70% in pool II (Fig. 1). The corresponding fractions in the PCP-protected batch were mixed into a single pool, $(I+II)^+$.

The material contained in pools I, II, and $(I+II)^+$ was individually submitted to automated sequence analysis. The three pools contained multiple overlapping sequences, indicating partial cleavage and incomplete separation, as has been observed with the other subunits (10–14). This pattern most probably arose from the hydrophobic character of the peptides studied. In each analysis, the same eight amino-terminal sequences could be identified, assigned on homology with the known sequence of the *T. californica* γ subunit (19) (Table 1). A significant background, already at cycle 1, suggested the presence of several minor cleavages giving rise to additional sequences, unidentifiable because of their low amount. The identified sequences extended, respectively, from Ser-126 (fragment $T_0$, see Fig. 2), Asn-194 ($T_1$), Asp-202 ($T_2$), Lys-218 ($T_3$, containing hydrophobic segment MI), Cys-252 ($T_4$, containing segment MII), Tyr-286 ($T_5$ containing segment MIII), Glu-429 ($T_6$), and Val-446 ($T_7$ containing segment MIV). Radioactivity was released at cycles 2, 6, 9, and 16 (Fig. 3). This release was decreased in the PCP-protected batch at cycles 2, 6, and 9, but not at cycle 16 (Fig. 3). Thus, only the labeled amino acids released at cycles 2, 6, and 9, which represented site(s) of PCP-sensitive incorporation of [$^3$H]CPZ, were considered further.

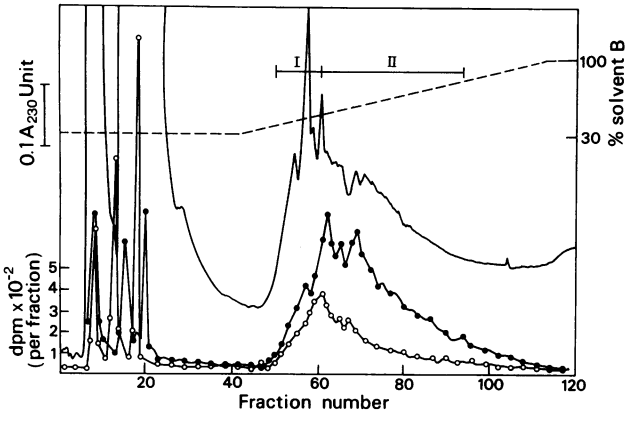


FIG. 1. Fractionation of the tryptic peptides from the carboxymethylated [$^3$H]CPZ-labeled γ chain. Purified labeled and carboxymethylated γ chain (30 nmol) from preparation 1 was suspended (1–2 mg of protein per ml) in 2 M urea/0.1 mM $CaCl_2$/50 mM $NH_4HCO_3$, pH 8.2, and trypsin was periodically added to a final 1:10 enzyme/substrate ratio over a 24-hr period at 37°C. The dried digest was dissolved in formic acid and injected on a $C_4$ Brownlee Labs Aquapore Butyl (7-μm, 220 × 4.6 mm) reversed-phase column equilibrated in 30% solvent B [solvent A: 0.1% trifluoroacetic acid; solvent B: 0.1% trifluoroacetic acid/90% (vol/vol) 1-propanol]. Elution was at 0.5 ml/min; the linear gradient is indicated by the broken line. The eluate was monitored by absorbance at 230 nm (—). Aliquots (5 μl) of the fractions collected every minute were subjected to liquid scintillation counting (●). Parallel treatment of the same amount of γ chain labeled by [$^3$H]CPZ in the presence of PCP produced a similar $A_{230}$ profile (data not shown) and the radioactivity profile shown here (○). Horizontal bars indicate the fractions mixed to form pools I and II.

As calculated from the specific radioactivity of the uncleaved γ subunit, the amount of radioactivity recovered at cycles 2, 6, and 9 in pool II corresponded to labeled amino acid amounts of at least 100, 30, and 40 pmol, respectively. These minimal values stand above PTH detection limit for identifiable sequences, indicating that the labeled residues belong to the sequences identified in pool II and, by extension, in pool I.

Fragments $T_1$ and $T_2$ display overlapping sequences, $T_2$ beginning eight residues after the amino terminus of $T_1$. Thus, the labeled amino acids cannot belong to peptide $T_2$ because, in that case, radioactivity release would also have been detected at cycles 10, 14, and 17. Similarly, no radioactive residue is located on $T_3$ (overlapping $T_2$), on $T_7$ (overlapping $T_6$), or at position 9 of $T_1$.

Moreover, the relative amounts of amino-terminal sequences and the amounts of radioactivity released were not similar in pools I and II. Radioactivity release at cycles 2, 6, and 9 increased ≈2-fold from pool I to pool II (Fig. 3), whereas the amounts of $T_0$, $T_6$, and $T_7$, respectively, decreased ≈3-, 7-, and 4-fold (Table 2). The labeled residues, thus, cannot belong to any of these three peptides.

In conclusion, the analysis of the tryptic digest of the carboxymethylated γ chain shows that three residues of this subunit incorporate [$^3$H]CPZ in a PCP-sensitive manner and

Table 1. Yields of phenylthiohydantoin (PTH)–amino acids upon automated sequence analysis of pool II·

| | PTH–amino acids, pmol × $10^{-1}$ | | | | | | | |
|---|---|---|---|---|---|---|---|---|
| Cycle | $T_0$ | $T_1$ | $T_2$ | $T_3$ | $T_4$ | $T_5$ | $T_6$ | $T_7$ |
| 1 | S + | N 56 | D 183 | K 184 | C | Y 56 | E 89 | V 150 |
| 2 | T 155 | Y 59 | D 134 | P 99 | T 155 | L 61 | Q 45 | I 55 |
| 3 | C | N 42 | T | L 100 | L 100 | I 77 | N 42 | D 58 |
| 4 | P 35 | W | D 99 | F 90 | S + | F 90 | D 99 | K 32 |
| 5 | I 63 | Q 13 | F 132 | Y 82 | I 63 | V 40 | S + | A 67 |
| 6 | A | L 15 | Q 64 | I 41 | S + | M 18 | G 16 | C |
| 7 | V 57 | T 9 | E 85 | I 56 | V 57 | F 65 | S + | F 65 |
| 8 | T 25 | K 11 | I 81 | N 36 | L 37 | V 43 | E 18 | W |
| 9 | Y 11 | D 3 | I 93 | I 93 | L 20 | S + | N 17 | I 93 |
| 10 | F 57 | D 12 | F 57 | I 50 | A 60 | M | E 5 | A 60 |
| 11 | P 8 | T | F 117 | A 66 | Q 20 | L 9 | N 6 | L 9 |
| 12 | F 35 | D 21 | L 68 | P 25 | T 35 | I 22 | W | L 68 |

The twelve first cycles of degradation over thirty cycles are shown (see Figs. 1–3). The amounts of PTH-derivatized amino acids (in one-letter code) obtained were calculated by constructing a plot of cycle vs. pmol released for each amino acid; the background was estimated by drawing a straight line through the low points. Due to lack of reliable standards, PTH-Ser groups could not be quantified and are indicated by + when detected. No value is indicated when residues expected according to the sequence could not be identified.

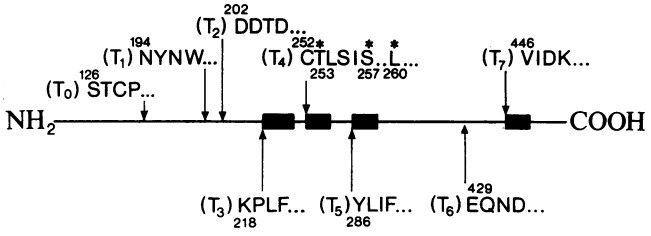


FIG. 2. Schematic drawing of the γ subunit, indicating the location of the sequenced peptides along the primary structure. Black boxes indicate the four hydrophobic segments (MI–MIV). Numbers indicate residue position within the *T. californica* sequence. Labeled amino acids (in one-letter code) are marked with an asterisk.

belong to the following set: Tyr-195, Trp-199 (residues 2 and 6 of $T_1$), Thr-253, Ser-257, Leu-260 (residues 2, 6, 9 of $T_4$, in segment MII), Leu-287, Met-291, Ser-294 (residues 2, 6, 9 of $T_5$, in segment MIII).

**Analysis of the Pyridylethylated γ Subunit Tryptic Fragments.** To distinguish among the possibilities for the labeling by [$^3$H]CPZ of peptides $T_1$, $T_4$, or $T_5$, we tried to modulate the efficiency of tryptic cleavage of the Lys-251–Cys-252 bond (beginning of $T_4$) by modifying the chemical treatment of the cysteine residues (pyridylethylation vs. carboxymethylation). The pyridylethylated γ subunit purified from preparation 2 (specific radioactivity, 1,200,000 dpm/nmol vs. 470,000 dpm/nmol for the PCP-protected batch) was cleaved with trypsin, and the digest was chromatographed under the same conditions as the carboxymethylated sample. Forty-five percent of the injected radioactivity was recovered associated with a broad $A_{210}$ peak eluting between 38 and 75% solvent B (data not shown). The corresponding material was pooled and submitted to automated sequence analysis. Among the several amino-terminal sequences present, $T_5$ could be unambiguously identified over at least eight cycles; in particular, PTH-Tyr, -Leu, -Ile, -Val, and -Met appearing, respectively, at cycles 1, 2, 3, 5, and 6 cannot be attributed to any other of the detected hydrophobic sequences. Similarly $T_1$ could be identified over at least 7 cycles (Table 3). $T_4$ (containing MII) was, however, no more detectable. Thus, in this pyridylethylated batch, cleavage of the Lys-251–Cys-252 bond occurred with a much lower yield than in the carboxymethylated batch. This change in cleavage efficiency could be due either to the different covalent modification of Cys-252 or to the low reproducibility of enzymatic cleavage of highly hydrophobic regions of the protein.

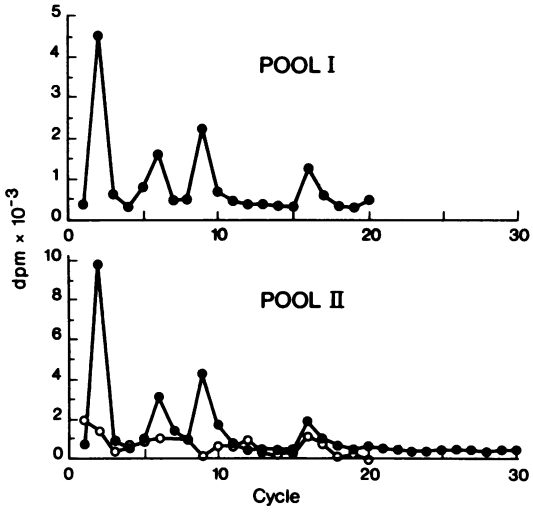


FIG. 3. Radioactivity released upon sequence analysis of tryptic peptides contained in pool I and pool II. The material contained in pools I and II was subjected to automated sequence analysis on a Beckman 890 C spinning cup sequencer for, respectively, 20 and 30 cycles, as described (11, 12). The loaded samples contained, respectively, 177,000 dpm (I) and 661,000 dpm (II). ●, Amount of radioactivity associated with each PTH released; ○, radioactivity released upon sequencing of the PCP-protected material (I+II)$^+$, in peptide amounts equivalent to that contained in pool II.

Table 2. Comparative distribution of γ-subunit tryptic fragments in pool I and pool II

| Peptide | Pool I, pmol | Pool II, pmol |
|---|---|---|
| $T_0$ | 960 (87) | 340 (94) |
| $T_1$ | NQ | 255 (95) |
| $T_2$ | 620 (94) | 1710 (92) |
| $T_3$ | 285 (98) | 1010 (92) |
| $T_4$ | 630 (90) | 800 (92) |
| $T_5$ | NQ | 570 (92) |
| $T_6$ | 3135 (89) | 410 (92) |
| $T_7$ | 3690 (89) | 885 (92) |

Initial amounts of degraded peptides in pmol and the repetitive yield (in parenthesis) were calculated by linear-regression analysis, excluding the residues shared by multiple sequences. As it is difficult to correct for overlaps in a sample with multiple sequences, calculated repetitive yields are probably overestimated, and errors of 20–30% are expected for initial amount values. Although the PTH-amino acids corresponding to $T_1$ and $T_5$ could be clearly identified upon degradation of pool I, their yields could not be fitted by linear-regression analysis, and these are thus indicated as not quantified (NQ).

As in the carboxymethylated batch, radioactivity was released at cycles 2, 6, and 9, but also at cycle 1 (Table 3). As seen by us and others (11–14), radioactivity release at cycle 1 upon sequencing takes place in an irreproducible fashion and is considered as artifactual. Furthermore, considering the different specific radioactivity of the two preparations, the amounts of labeled amino acid released at cycles 2, 6, and 9 dramatically decreased (80-, 15-, and 30-fold, respectively) from the carboxymethylated pool II to the pyridylethylated sample (Table 3 and Fig. 3) and likely fell under PTH-detection limit for identifiable sequences. As a consequence, $T_1$ and $T_5$ cannot be labeled by [$^3$H]CPZ because from the carboxymethylated pool II to the pyridylethylated sample

Table 3. Yields of PTH-amino acids corresponding to peptides $T_1$ and $T_5$ upon automated sequence analysis of tryptic fragments of the pyridylethylated γ subunit

| | PTH-amino acids, pmol | | |
|---|---|---|---|
| Cycle | $T_1$ | $T_5$ | dpm released |
| 1 | N 240 | Y 384 | 3070 |
| 2 | Y 130 | L 338 | 2950 |
| 3 | N 108 | I 288 | 1725 |
| 4 | W | F 806 | 1430 |
| 5 | Q 38 | V 316 | 1435 |
| 6 | L 72 | M 98 | 4020 |
| 7 | T 10 | F 37 | 2975 |
| 8 | K | V 35 | 2570 |
| 9 | D | S | 3010 |
| 10 | D 32 | M | 2530 |
| Initial amount | 215 | 890 | |
| Repetitive yield | 76% | 72% | |

Purified labeled and pyridylethylated γ chain (4 nmol) of preparation 2 was treated with trypsin (see Fig. 1). The digest was purified by reversed-phase HPLC (see text), and a sample of the eluate (1,950,000 dpm) was subjected to automated sequence analysis on an Applied Biosystems 470 A sequencer coupled on-line to a 120A PTH analyzer. Asparagine (cycle 3) and phenylalanine (cycle 7) being shared by multiple sequences (data not shown) were not taken into account for quantification. Peptides $T_2$, $T_3$, $T_6$, and $T_7$ were also detected during this sequence (between 300 and 700 pmol).

their amount increased (≈1.5-fold for $T_5$, Tables 2 and 3) or remained constant ($T_1$).

In summary, analysis of the tryptic peptides generated after carboxymethylation of the γ subunit showed that the [$^3$H]-CPZ labeling is located on either fragment $T_1$, $T_4$, or $T_5$. Comparison with the pyridylethylated batch rules out the labeling of $T_1$ and $T_5$. The only remaining possibility is, thus, labeling of $T_4$; this fragment was not identified at the PTH level upon sequencing of the pyridylethylated batch, which agrees with the fact that the low level of label released during this degradation corresponds to a peptide amount standing under PTH-detection limit for identifiable sequences.

In conclusion, sequence analysis of the γ-subunit tryptic peptides demonstrates that three amino acids from $T_4$ incorporate [$^3$H]CPZ in a PCP-sensitive manner and are Thr-253 (cycle 2), Ser-257 (cycle 6), and Leu-260 (cycle 9) in the MII hydrophobic segment.

## DISCUSSION

Tryptic cleavage under different conditions of the [$^3$H]CPZ-labeled γ subunit generated distinct sets of partially resolved hydrophobic peptides and led to the identification of three residues labeled in a PCP-sensitive manner, Thr-253, Ser-257, and Leu-260, all belonging to the hydrophobic segment MII.

**Structure of the High-Affinity Site for NCBs.** On the other subunits of the AcChoR, [$^3$H]CPZ was already shown to label MII at positions homologous to that of Ser-γ257—namely, serines-α248, -β254, and -δ262 (10–12). Additional labeling was also demonstrated for Leu-β257 homologous to Leu-γ260 (11). The present results confirm that homologous regions from the different subunits contribute to the unique high-affinity site for NCBs (4). Interestingly, however, although homologous Leu-β257 and -γ260 are labeled by [$^3$H]CPZ, no labeling was detected on the leucines at the corresponding position on the MII segment of the α and δ subunits (10, 12). Similarly, although Thr-γ253 incorporated [$^3$H]CPZ, the homologous residues on the other subunits were not labeled (10–12). This difference in labeling pattern between subunits may reflect the existence of a discrete local asymmetry at the level of the [$^3$H]CPZ multi-subunit site. Such deviation from perfect symmetry, already suggested by the only partial sequence identity of AcChoR subunits, may also account for the different labeling patterns seen with other photoactivatable NCBs (5) or different *Torpedo* species (20).

The respective position on the MII sequence of the three [$^3$H]CPZ-labeled amino acids is consistent with the organization of MII into an α-helix (see also refs. 11 and 32). Indeed, in such a configuration the α carbons of Ser-γ257 and Leu-γ260 are predicted to lie, respectively, at 1.1 and 1.9 helix turn from the α carbon of Thr-γ253, and, as a consequence, the three labeled residues would be aligned on adjacent turns of the α-helix. The distance between the α carbons of Thr-γ253 and Leu-γ260 would then be 10.7 Å, a distance compatible with the dimensions of CPZ deduced from its crystal structure (21). The labeling of amino acids probably distributed over a 360° angle and neighboring α-helical turns may also reflect multiple binding modes of [$^3$H]CPZ to its site and/or different photoactivation pathways of the CPZ molecule (22).

**Role of the γ Subunit in Desensitization.** In the present study, the labeling by [$^3$H]CPZ was performed in the presence of 1 mM carbamoylcholine, which stabilizes the AcChoR in its desensitized state. The distinct labeling pattern of the γ subunit compared with that of the other chains may be related to its particular behavior in the permeability response of the AcChoR. Indeed, upon [$^3$H]CPZ labeling of the desensitized AcChoR, the γ subunit is among all subunits the one that incorporates the lowest amounts of radioactivity (4), whereas it incorporates more radioactivity than the other subunits upon labeling of the AcChoR in the open-channel state (6). Such a differential labeling of the open and desensitized states is not seen with the other subunits. It might reflect the displacement of the γ subunit slightly away from the receptor axis upon desensitization, noticed with tubular crystals of AcChoR (23), which could render the γ subunit less accessible to [$^3$H]CPZ. Furthermore, electrophysiological studies of hybrid *Torpedo*–cat AcChoR expressed in *Xenopus* oocytes (24) reveal a definite role of the γ subunit in the desensitization process.

**Organization of the AcChoR Ion Channel.** From electrophysiological recordings, some NCBs (for review, see refs. 7 and 8), including CPZ and PCP (25), were suggested to sterically block ion flux by plugging the ionic channel. This hypothesis is reinforced by rapid-mixing and photolabeling experiments in the millisecond time range (6) and by the demonstration that channel-permeant cations competitively block binding of ethidium to the high-affinity site for NCBs (9).

Since the initial demonstration of the participation of the MII segment to the high-affinity site for NCBs (10), additional evidence, mainly from mutagenesis experiments, has provided further support to the proposal (10) that this segment is, indeed, part of the ion channel: (*i*) exchange of a region of the δ subunit comprising MII and a portion located between MII and MIII alters the rate of regulation of ion transport through the open channel (15); (*ii*) mutation of the rings of negatively charged amino acids framing MII changes ionic channel conductance (16); and finally (*iii*) mutation in mouse AcChoR of serine residues homologous to those labeled by [$^3$H]CPZ creates a change of affinity of the open-channel blocker QX-222 (17), and, when three of them are mutated, decreases outward currents (see also ref. 32).

The simplest model accounting for this set of results is that the MII segments, organized in α-helices, are pseudosymmetrically arranged around the AcChoR axis and compose the walls of the ion channel (Fig. 4). Accordingly, in such a configuration, on each subunit the residues labeled by [$^3$H]-CPZ and the negatively charged amino acids framing MII would be aligned along one face of the α-helix (26) and thus would all point toward the channel lumen.

If one assumes, as a working hypothesis, that CPZ can reach its site from the extracellular part of the channel, the MII helices should be tilted with respect to the central axis (26), forming a truncated cone with its tightest end towards the cytoplasm. This narrow part, sufficient for ions passage, would constitute the NCB high-affinity site to which [$^3$H]CPZ binds. Length of the narrowest cross section of the ion channel—i.e., the main cation-binding site, has been estimated by measurements of streaming potential, to be ≈3–6 Å (27) and corresponds approximately to one α-helix turn. Here we show that on the γ subunit, the site for [$^3$H]CPZ extends over two α-helix turns, thus covering more than strictly the length of the narrowest part of the channel.

The studies with photoactivatable NCBs (10–14 and this study) and mutagenesis experiments (17) have singled out three "rings" of amino acids as plausibly participating in the cation-binding site within the channel (Fig. 4): the ring of serines homologous to Ser-γ257, another polar ring of amino acids at positions homologous to Thr-γ253, and one "hydrophobic" leucine ring at a position homologous to Leu-γ260. Residues from these rings are conserved at the same position (or replaced by another polar amino acid for threonine or serine) in all but a few AcChoR subunits cloned, and even in the γ-aminobutyric acid type A and glycine receptors for Leu-γ260 and Ser-γ257 (for review, see ref. 28). These rings may, thus, be of general importance for ion transport. In particular, a possibility to consider (29) is that the serine and

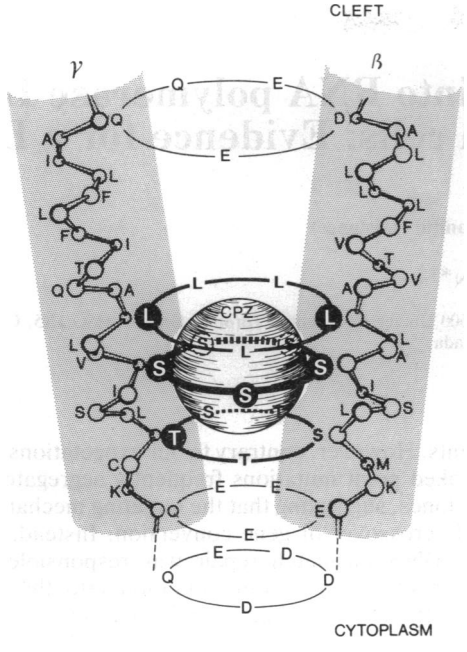


FIG. 4. A model of the high-affinity site for CPZ within the AcChoR ion channel. The MII segments, arranged as transmembrane α-helices are quasisymmetrically organized around the central axis of the molecule and are tilted with respect to this axis (26). Subunits are tentatively ordered as in ref. 31; Segments MII of the β and γ subunits are depicted in more detail. The scheme displays the α carbons of the considered amino acids. The amino acids (in one-letter code) labeled by [$^3$H]CPZ in a PCP-sensitive manner are circled in black. Mutagenesis experiments (16) show that the "negatively charged rings" (QED) framing MII may also play a role in ion transport. No hypothesis is advanced concerning the configuration of CPZ in its site, which is represented as a sphere.

threonine rings contribute to dehydration of permeating ions by substituting for some of the water molecules of their hydration shell (30). Future experiments, in particular by site-directed mutagenesis, may help define the role of the three rings in cation transport through the AcChoR channel.

We thank P. Ascher, A. Menez, A. Bessis, A. Devillers-Thiéry, J. Hill, A. Klarsfeld, and R. Laufer for critically reading the manuscript; we also thank H. Nuret and N. Savatier for technical assistance. This work was supported by research grants from the Association Française contre les Myopathies, the Collège de France, the Centre National de la Recherche Scientifique, the Ministère de la Recherche, Institut National de la Sauté et de la Recherche Médicale (Contract 872 004) and the Direction des Recherches Etudes et Techniques (Contract 87/211). F.R. was supported by Fondation Roux and J.-L.G. was supported by the Association Française contre les Myopathies.

1. Changeux, J.-P., Devillers-Thiéry, A. & Chemouilli, P. (1984) *Science* **225,** 1335–1345.
2. Mishina, M., Kurosaki, T., Tobimatsu, T., Morimoto, Y., Noda, M., Yamamoto, T., Terao, M., Lindstrom, J., Takahashi, T., Kuno, M. & Numa, S. (1984) *Nature (London)* **307,** 604–608.
3. Hucho, F. (1986) *Eur. J. Biochem.* **158,** 211–226.
4. Heidmann, T., Oswald, R. E. & Changeux, J.-P. (1983) *Biochemistry* **22,** 3112–3127.
5. Oswald, R. & Changeux, J.-P. (1981) *Proc. Natl. Acad. Sci. USA* **78,** 3925–3929.
6. Heidmann, T. & Changeux, J.-P. (1986) *Biochemistry* **25,** 6109–6113.
7. Neher, E. & Steinbach, J. H. (1978) *J. Physiol. (London)* **277,** 153–176.
8. Adams, P. R. (1981) *J. Membr. Biol.* **58,** 161–174.
9. Herz, J. M., Erlanger, T. P. & Kolb, S. J. (1989) *Soc. Neurosci. Abstr.* **15,** 969.
10. Giraudat, J., Dennis, M., Heidmann, T., Chang, J. Y. & Changeux, J.-P. (1986) *Proc. Natl. Acad. Sci. USA* **83,** 2719–2723.
11. Giraudat, J., Dennis, M., Heidmann, T., Haumont, P.-Y., Lederer, F. & Changeux, J.-P. (1987) *Biochemistry* **26,** 2410–2418.
12. Giraudat, J., Galzi, J.-L., Revah, F., Changeux, J.-P., Haumont, P.-Y. & Lederer, F. (1989) *FEBS Lett.* **253,** 190–198.
13. Oberthür, W., Muhn, P., Baumann, H., Lottspeich, F., Wittmann-Liebold, B. & Hucho, F. (1986) *EMBO J.* **5,** 1815–1819.
14. Hucho, F. L., Oberthür, W. & Lottspeich, F. (1986) *FEBS Lett.* **205,** 137–142.
15. Imoto, K., Methfessel, C., Sakmann, B., Mishina, M., Mori, Y., Konno, T., Fukuda, K., Kurasaki, M., Bujo, H., Fujita, Y. & Numa, S. (1986) *Nature (London)* **324,** 670–674.
16. Imoto, K., Busch, C., Sakmann, B., Mishina, M., Konno, T., Nakai, J., Bujo, H., Mori, Y., Fukuda, K. & Numa, S. (1988) *Nature (London)* **335,** 645–648.
17. Leonard, R. J., Labarca, C. G., Charnet, P., Davidson, N. & Lester, H. A. (1988) *Science* **242,** 1578–1581.
18. Tarr, G. E. (1986) in *Methods of Protein Microcharacterization* ed. Shively, J. E. (Humana, Clifton, NJ), p. 162.
19. Noda, M., Takahashi, H., Tanabe, T., Toyosato, M., Kikyotani, S., Furutani, Y., Hirose, T., Takashima, H., Inayama, S., Miyata, T. & Numa, S. (1983) *Nature (London)* **302,** 528–532.
20. Haring, R., Kloog, Y., Kalir, A. & Sokolovsky, M. (1983) *Biochem. Biophys. Res. Commun.* **113,** 723–729.
21. McDowell, J. J. H. (1969) *Acta Cryst. B* **25,** 2175–2181.
22. Huang, C. L. & Sands, F. L. (1964) *J. Chromatogr.* **13,** 246–249.
23. Unwin, N., Toyoshima, C. & Kubalek, E. (1988) *J. Cell Biol.* **107,** 1123–1138.
24. Sumikawa, K. & Miledi, R. (1989) *Proc. Natl. Acad. Sci. USA* **86,** 367–371.
25. Changeux, J.-P., Pinset, C. & Ribera, A. B. (1986) *J. Physiol. (London)* **378,** 497–513.
26. Furois-Corbin, S. & Pullman, A. (1989) *Biochim. Biophys. Acta* **984,** 339–350.
27. Dani, J. A. (1989) *J. Neurosci.* **9,** 884–892.
28. Unwin, N. (1989) *Neuron* **3,** 665–676.
29. Changeux, J.-P. (1990) *Fidia Research Foundation Neuroscience Award Lectures* (Raven, New York), Vol. 4, in press.
30. Hille, B. (1984) *Ionic Channel of Excitable Membranes* (Sinauer, Sunderland, MA).
31. Kubalek, E., Ralston, S., Lindstrom, J. & Unwin, N. (1987) *J. Cell Biol.* **105,** 9–18.
32. Charnet, P., Labarca, C., Leonard, R. J., Vogelaar, N. J., Czyzyk, L., Gouin, A., Davidson, N. & Lester, H. A. (1990) *Neuron* **2,** 87–95.